Genomic Profiling of MicroRNAs in Bladder Cancer: miR-129 Is Associated with Poor Outcome and Promotes Cell Death *In vitro*

Lars Dyrskjøt,[1] Marie S. Ostenfeld,[1] Jesper B. Bramsen,[3] Asli N. Silahtaroglu,[6] Philippe Lamy,[1] Ramshanker Ramanathan,[1] Niels Fristrup,[1] Jens L. Jensen,[4] Claus L. Andersen,[1] Karsten Zieger,[1,2] Sakari Kauppinen,[6,7] Benedicte P. Ulhøi,[5] Jørgen Kjems,[3] Michael Borre,[2] and Torben F. Ørntoft[1]

[1]Molecular Diagnostic Laboratory, Department of Molecular Medicine, and [2]Department of Urology, Aarhus University Hospital; Departments of [3]Molecular Biology and [4]Theoretical Statistics and Mathematical Sciences, University of Aarhus; [5]Institute of Pathology NBG, Aarhus Hospital, Aarhus, Denmark; [6]Wilhelm Johannsen Centre for Functional Genome Research, Department of Cellular and Molecular Medicine, Copenhagen, Denmark; and [7]Santaris Pharma, Hørsholm, Denmark

Abstract

microRNAs (miRNA) are involved in cancer development and progression, acting as tumor suppressors or oncogenes. Here, we profiled the expression of 290 unique human miRNAs in 11 normal and 106 bladder tumor samples using spotted locked nucleic acid–based oligonucleotide microarrays. We identified several differentially expressed miRNAs between normal urothelium and cancer and between the different disease stages. miR-145 was found to be the most down-regulated in cancer compared with normal, and miR-21 was the most up-regulated in cancer. Furthermore, we identified miRNAs that significantly correlated to the presence of concomitant carcinoma *in situ*. We identified several miRNAs with prognostic potential for predicting disease progression (e.g., miR-129, miR-133b, and miR-518c*). We localized the expression of miR-145, miR-21, and miR-129 to urothelium by *in situ* hybridization. We then focused on miR-129 that exerted significant growth inhibition and induced cell death upon transfection with a miR-129 precursor in bladder carcinoma cell lines T24 and SW780 cells. Microarray analysis of T24 cells after transfection showed significant miR-129 target down-regulation (P = 0.0002) and pathway analysis indicated that targets were involved in cell death processes. By analyzing gene expression data from clinical tumor samples, we identified significant expression changes of target mRNA molecules related to the miRNA expression. Using luciferase assays, we documented a direct link between miR-129 and the two putative targets GALNT1 and SOX4. The findings reported here indicate that several miRNAs are differentially regulated in bladder cancer and may form a basis for clinical development of new biomarkers for bladder cancer. [Cancer Res 2009;69(11):4851–60]

Introduction

Bladder cancer is a common malignancy in men in economically advanced nations. The disease presents in two different forms: non–muscle-invasive tumors (stage Ta and T1) and muscle-invasive cancers (stage T2-4). Non–muscle-invasive tumors form a heterogeneous group, spanning from completely benign, noninvasive papillary tumors that rarely progress, to papillary lamina propria–invasive high-grade tumors, which progress to muscle-invasive cancer in up to 60% at long-term follow-up (1). Several high-throughput studies have thus far focused on delineating genomic changes and gene expression in the different stages of bladder cancer development and progression (2). Interestingly, recent studies have documented a link between the expression of microRNAs (miRNA) and cancer pathogenesis for other types of cancer, such as glioblastoma and colorectal, lung, breast, hepatic, and pancreatic cancer (3–8). However, only few reports have described miRNA expression in bladder cancer (9, 10). miRNAs associated with disease outcome in bladder cancer have not been described previously.

miRNAs have emerged as central regulators of development, differentiation, and cancer (11). The implication of miRNAs in tumorigenesis first came from the observation that a common deletion in human chronic lymphocyte leukemia (CLL) harbors the miRNA genes encoding miR-15 and miR-16, the loss of which is seen in ~65% of all cases of CLL (12). Under normal conditions, these miRNAs target the B-cell lymphoma 2 (Bcl-2) transcript and hereby reduce the level of antiapoptotic Bcl-2, leading to a steady-state level of apoptosis (13). Thus, in CLL patients, the loss of miR-15 and miR-16 was found to be correlated with increased Bcl-2 expression and decreased apoptosis, leading to expansion of nondividing B cells (13). In breast cancer, a differential expression pattern of 2 to 11 miRNAs was found to discriminate between differential estrogen and progesterone receptor expression, as well as lymph node metastasis, vascular invasion, proliferation index, ERB2 expression, and p53 expression (3). Furthermore, it has been shown that expression of miR-335 and miR-126 is lost in tumors from breast cancer patients with poor distal metastasis-free survival (14). Expression of miR-155 in lung cancer patients was found to be associated with poor prognosis (15). In another recent study, distinct miRNA profiles found in different types of cancer suggested that miRNAs can accurately identify the tissue origin of cancer and thus be exploited in the classification of tissue origin of metastatic cancer of unknown primary origin (16).

Here, we profiled the expression of miRNAs in 106 bladder cancers and 11 normal samples using in-house spotted locked nucleic acid (LNA)–based oligonucleotide microarrays. We identified several miRNAs aberrantly expressed between different stages of bladder cancer, and miRNAs associated with disease progression

Note: Supplementary data for this article are available at Cancer Research Online (http://cancerres.aacrjournals.org/).

Requests for reprints: Lars Dyrskjøt, Molecular Diagnostic Laboratory, Department of Molecular Medicine, Aarhus University Hospital, Skejby, DK-8200 Aarhus N, Denmark. Phone: 45-8949-9420; E-mail: lars@ki.au.dk.

doi:10.1158/0008-5472.CAN-08-4043

and outcome. We investigated the function of the progression marker miR-129 *in vitro* using cell viability and cell death assays and by analyzing the changes in miR-129 target expression *in vitro* and in additional clinical tumor samples.

Materials and Methods

Cell culture and transfections. Human urinary bladder transitional cell carcinoma (T24, SW780, HT1376, RT4, and J82) and immortalized human bladder epithelium (HU609 and HCV29) cells were propagated in DMEM (Invitrogen) supplemented with 10% heat-inactivated FCS and antibiotics (complete medium) at 37°C in a humidified air atmosphere at 5% CO_2. Precursor and scrambled miRNAs (Ambion, Inc.) and miR LNA knockdown molecules (Exiqon) were reverse transfected at indicated final concentrations using Lipofectamine 2000 (Invitrogen) according to the manufacturer's guidelines. The cells were seeded after addition of the transfection mix into the wells, and the medium was changed to RPMI 1640 supplemented with 10% heat-inactivated FCS and antibiotics ~8 h after transfection.

Patient material. Tumor samples were obtained directly from surgery after removal of the necessary amount of tissue for routine pathology examination. All tumors were graded by the Bergkvist classification system (17). Informed written consent was obtained from all patients, and research protocols were approved by the ethical committee of Aarhus County. The tumors were frozen at −80°C in a guanidinium thiocyanate solution and RNA was extracted from the samples using a standard Trizol RNA extraction method (Invitrogen).

Detection of cell viability and cell death. The viability and death of the cells were analyzed by 3-(4,5-dimethylthiazol-2-yl)-2,5-diphenyltetrazolium bromide (MTT; Sigma-Aldrich) reduction and lactate dehydrogenase (LDH; cytotoxicity detection kit from Roche) assays essentially as described (18). The LDH release was calculated as follows: % LDH release = LDH medium / (LDH medium + LDH lysate).

Microarray expression profiling and data analysis. miRNA microarrays were produced using an oligonucleotide probe library (mercury LNA array ready to spot v.7.1) purchased from Exiqon. miRNA microarrays were spotted, hybridized, and scanned and samples were labeled as described (19). We used TIGR Spotfinder 2.23 software to generate raw intensity data, which were LOWESS (global) normalized using TIGR MIDAS 2.19 software (20). Average $\log_2$ ratios were calculated from the normalized data based on the two measurements of each miRNA. For analysis of microarray data, we used significance analysis of microarrays (SAM) implemented in TIGR MEV 4.0 software (20). Two data sets were created: one where a background filter (1*BG+2*SD) was applied in MIDAS and one without background filtering. The background-filtered data set was used to determine in how many samples each probe was detected above background. All analyses were performed on the data set where no filter was applied. The percentage detected calls are listed for each probe in Tables 1 and 2. For all analyses, we performed 1,000 permutations of the data to select differentially expressed miRNA based on false discovery rate (FDR) estimations. Data were median centered and normalized before hierarchical cluster analysis by GeneCluster. TreeView software was used for visualization of the data. Affymetrix human exon ST 1.0 arrays were used for measuring gene expression at 24 and 48 h following pre-miR-129 transfection of T24 cells as previously described (21). itPLIER normalization and generation of gene expression measures was performed in GeneSpring GX 10.0. Gene networks affected by miR-129 transfection were analyzed by Ingenuity Pathway Analysis (IPA).

Real-time reverse transcription-PCR miRNA expression profiling. We used Taqman PCR assays (Applied Biosystems) for measuring the miRNA and mRNA expression quantitatively. PCR assays were performed as described by the manufacturer using an ABI 7500 PCR system. For normalization, we used RNU6B or UBC.

***In situ* detection of miRNAs.** *In situ* detection of miRNAs was performed on 10-μm frozen tissue sections from freshly removed tumors. Sections were fixed in 4% paraformaldehyde, acetylated, and prehybridized in hybridization solution (50% formamide, 5× SSC, 0.5 mg/mL yeast tRNA, 1× Denhardt's solution) for 30 min before hybridization. Probe (3 pmol; LNA-modified and FITC-labeled oligonucleotide; Exiqon) complementary to miR-21, miR-145, and miR-129 was hybridized to the sections for 1 h at 25°C lower than predicted T_m of the probe. After posthybridization washes, *in situ* hybridization signals were detected using the tyramide signal amplification system (Perkin-Elmer) according to the manufacturer's instructions. Slides were mounted in ProLong Gold containing 4′,6-diamidino-2-phenylindole (DAPI; Invitrogen) and analyzed with an Olympus MVX10 microscope equipped with a charge-coupled device camera and Olympus CellP software.

Target prediction and regulation *in vitro* and *in vivo*. We investigated the target regulation upon miR-129 transfection of T24 cells. Genes differentially expressed >1.4-fold between cells transfected with miR-129 and cells transfected with a scrambled sequence were considered differentially expressed. Genes were considered expressed above background if the intensity was above 8 ($\log_2$ scale) in untreated T24 cells. miR-129 targets were identified from the TargetScan prediction algorithm. In addition, we used previously published gene expression data sets to investigate changes in transcript levels of miRNA targets between the groups: normal versus cancer, Ta versus T2, no carcinoma *in situ* (CIS) versus CIS, and no progression versus progression (22–24). Genes were defined as being up-regulated or down-regulated when regulated >2-fold between the groups investigated and when the difference was statistically significant ($P < 0.01$, Student's t test). Only genes present in the databases of the prediction algorithms TargetScan (25) and PicTar (26) were considered. We considered a mRNA to be a target if it was found among the predicted targets in at least one of the two algorithms used. TargetScan differentiates between miRNAs that are conserved and miRNAs that are poorly conserved in different organisms. For the conserved miRNAs, only the conserved predicted targets were considered as targets, whereas for the poorly conserved miRNAs, all the predicted targets, poorly conserved and conserved, were considered as targets. We only investigated miRNAs found in one of the two algorithm databases (Supplementary Table S1).

miR-129 target validation. A partial 3′-untranslated region (ΔUTR) sequence of 400 to 800 bp from *BRPM2, ETV6, GALNT1,* and *SOX4* containing the putative miR-129 target sites was inserted into the *Xho*I/*Not*I site of the psiCHECK2 vector (Promega). The corresponding mutant UTRs for each gene were created by substituting the putative miR-129 target sites (positions complementary to the miR-129 seed regions only) with a *Pvu*I restriction site by an overlapping PCR approach; four, three, two, and one putative target sites were mutated for *SOX4, GALNT1, ETV6*, and *BRPM2*, respectively (see Supplementary Table S2 for primer sequences). HEK293 cells were cotransfected in 48-well format with 0.025 μg psiCHECK-UTR DNA and 50 nmol/L pre-miRNA (hsa-miR129-5p and Pre-miRNA Precursor Negative Control 1; both Ambion) using Mirus TransIT LT1 and TransIT TKO (Mirus Corp.) in 250 μL of 10% FCS in RPMI 1640 per well. The luciferase activity was measured 30 h after transfection and normalized using the Dual-Luciferase Reporter Assay System (Promega) on a FLUOstar luminometer (BMG Labtech). The experiment was performed in triplicates and the relative rluc/fluc value for each of the four wild-type UTR constructs was normalized to the relative rluc/fluc value of the corresponding mutated UTR.

Statistical procedures. Kaplan-Meier estimates, univariate and multivariate Cox regression analyses, and logistic regression analyses were done using the STATA 10.0 statistical analysis software. Maximum likelihood classification procedures were performed as previously described (27). χ^2 test was used to test for difference in expression between nontarget and target genes.

Results

We profiled the expression of 290 unique human miRNA genes in tumorigenic cell lines (T24, SW780, RT4, HT1376, and J82) and in immortalized urothelial cell lines (HCV29 and HU609).

Furthermore, we analyzed the expression in 11 biopsies of normal urothelium obtained from healthy individuals and in 30 Ta tumors, 49 T1 tumors, and 27 T2-4 tumors. Patients with nonprogressing Ta and T1 tumors had a median follow-up time of 64 months and patients with progressing tumors had a median time to progression of 10 months. Clinical and histopathologic parameters for the patients included in this study are listed in Supplementary Table S3.

Table 1. miRNAs differentially expressed between normal bladder tissue and bladder cancer and between Ta and T2-4 tumors

ID*	miRNA	Fold change †	P ‡	Detected (%)§	Chromosome location
miRNAs up-regulated in cancer					
13132	miR-519e*	1.7	4.1E−08	93	19q13.41
10986	miR-193a-3p	2.0	2.8E−07	61	17q11.2
5740	miR-21	3.7	2.9E−07	87	17q23.3
11008	miR-20a	2.1	7.8E−06	70	13q31.3
10993	miR-198	2.0	2.5E−05	95	3q13.33
11142	miR-510	2.6	2.7E−05	88	Xq27.3
10978	miR-184	1.9	7.5E−05	75	15q25.1
11124	miR-492	2.6	9.4E−05	97	12q22
miRNAs down-regulated in cancer					
13179	miR-455-5p	−2.6	4.4E−11	45	9q32
13177	miR-143	−2.6	6.9E−09	74	5q33.1
10951	miR-145	−7.0	2.1E−08	93	5q33.1
10930	miR-126*	−2.0	1.8E−07	43	9q34.3
11030	miR-26a	−1.6	4.4E−06	73	3p22.2/12q14.1
10929	miR-125b	−2.3	7.2E−06	91	11q24.1/21q21.1
11130	miR-498	−1.9	2.1E−05	90	19q13.41
11121	miR-489	−1.9	2.8E−05	41	7q21.3
11135	miR-503	−2.3	4.1E−05	99	Xq26.3
11039	miR-29a	−1.7	4.3E−05	79	7q32.3
11043	miR-302b	−1.3	4.6E−05	20	4q25
11041	miR-29c	−2.0	5.8E−05	96	1q32.2
miRNAs up-regulated in T2-4 compared with Ta					
11135	miR-503	2.5	1.1E−08	99	Xq26.3
10934	miR-129-5p	2.6	2.3E−08	97	7q31/11p11.2
11054	miR-320a	1.9	7.3E−08	95	8p21.3
10987	miR-193b	1.9	2.8E−07	37	16p13.12
13180	miR-483-3p	2.3	5.2E−07	77	11p15.5
11130	miR-498	1.6	1.2E−06	90	19q13.41
11151	miR-516b	1.5	1.5E−06	43	19q13.41
11060	miR-328	1.5	3.0E−06	41	16q22.1
11086	miR-373*	1.9	1.5E−05	91	19q13.41
13132	miR-519e*	1.4	1.5E−05	93	19q13.41
11176	miR-526b	1.9	2.0E−05	48	19q13.41
11035	miR-296-5p	1.5	2.6E−05	99	20q13.32
11122	miR-490-3p	1.3	3.5E−05	24	7q33
11121	miR-489	1.3	1.0E−04	41	7q21.3
miRNAs down-regulated in T2-4 compared with Ta					
13141	miR-18b	−1.5	1.3E−07	79	Xq26.2
11019	miR-219-5p	−2.1	4.7E−06	68	6q21.32/9q34.11
11182	miR-98	−1.7	5.4E−06	85	Xp11.22
10946	miR-141	−2.8	1.0E−05	78	12p13.31
11002	miR-200c	−2.0	4.3E−05	76	12p13.31
13126	miR-191*	−1.7	5.0E−05	91	3q21.31
11004	miR-203	−2.3	5.4E−05	72	14q32.33
11073	miR-34b*	−1.2	8.7E−05	9	11q23.1

NOTE: Only the most significant are listed ($P < 0.0001$, Student's t test).

*Probe ID from LNA library 208010V7.1 (Exiqon).

†Fold change values were generated from the median expression of the miRNAs in the groups compared. The reciprocal number multiplied by −1 was used for down-regulated genes.

‡Student's t test P values.

§Percentage of samples in which the miRNA is detected above the background filter.

Table 2. miRNAs differentially expressed between nonprogressing and progressing tumors and between tumors with and without concomitant CIS

ID*	miRNA	Fold change†	P‡	Detected (%)§	Chromosome location
miRNAs up-regulated in progressing tumors					
10934	miR-129-5p	1.6	0.001	97	7q31/11p11.2
13131	miR-518c*	1.2	0.002	94	19q13.41
5560	miR-185	1.3	0.003	98	22q11
10939	miR-133b	1.4	0.003	19	6p12.2
11086	miR-373*	1.2	0.005	91	19q13.41
11054	miR-320a	1.4	0.008	95	8p21.3
10951	miR-145	1.4	0.022	93	5q33.1
miRNAs down-regulated in progressing tumors					
11041	miR-29c	−1.5	0.001	96	1q32.2
11040	miR-29b	−1.7	0.001	89	1q32.2/7q32.3
11039	miR-29a	−1.4	0.003	79	7q32.3
11075	miR-361-5p	−1.2	0.005	42	Xq21.2
11004	miR-203	−1.7	0.004	72	14q32.33
11006	miR-205	−2.6	0.014	56	1q32.2
miRNAs up-regulated in tumors with concomitant CIS					
11135	miR-503	1.9	<0.001	99	Xq26.3
11130	miR-498	1.5	0.001	90	19q13.41
10934	miR-129-5p	1.9	0.001	97	7q31/11p11.2
11086	miR-373*	1.5	0.002	91	19q13.41
13180	miR-483-3p	1.5	0.009	77	11p15.5
11054	miR-320a	1.2	0.014	95	8p21.3
11248	miR-451	1.5	0.015	87	17q11.2
10997	miR-19a	1.1	0.050	28	13q31.3
miRNAs down-regulated in tumors with concomitant CIS					
11006	miR-205	−2.6	<0.001	56	1q32.2
13126	miR-191*	−1.5	0.001	91	3p21.31
11097	miR-382	−1.4	0.001	61	14q32.31
10931	miR-127-3p	−1.6	0.001	97	14q32.31
11041	miR-29c	−1.7	0.001	96	1q32.2
13127	miR-200a*	−1.4	0.002	61	1p36.33
11052	miR-31	−1.3	0.002	30	9p21.3
11043	miR-302b	−1.2	0.003	20	4q25
11070	miR-345	−1.4	0.004	26	14q32.2
13183	miR-487a	−1.5	0.006	34	14q32.31

*Probe ID from LNA library 208010V7.1 (Exiqon).
†Fold change values were generated from the median expression of the miRNAs in the groups compared. The reciprocal number multiplied by −1 was used for down-regulated genes.
‡Student's t test P values.
§Percentage of samples in which the miRNA is detected above the background filter.

Unsupervised hierarchical cluster analysis of cell lines, normal urothelium biopsies, and bladder tumor biopsies. Hierarchical cluster analysis of the 122 miRNAs with expression above background in minimum 25% of samples separated the samples into one arm (Supplementary Fig. S1) with an overrepresentation of Ta tumors and T1 tumors without subsequent progression and another arm with an overrepresentation of T1 tumors with subsequent progression ($P = 0.002$, χ^2 test) clustering among the T2-4 tumors. Overall, the expression of miRNA in the cell lines and the immortalized normal urothelial cells resembled the expression of miRNA in Ta tumors. Furthermore, the cluster analysis showed very little variation in miRNA expression between the different immortalized and tumorigenic cell lines.

miRNAs differentially expressed between normal and cancer and between different stages of cancer. We delineated miRNAs differentially expressed between normal urothelium and tumor samples and between Ta, T1, and T2-4 stages using SAM (0% FDR as cutoff). The 73 probes against human miRNAs that showed significant differential expression are shown in Fig. 1*A*. Several miRNAs were found to be specifically associated with normal tissue, Ta tumors, and T2-4 tumors; however, the T1 tumors showed expression similarities to either Ta or T2-4 tumors. The most significantly regulated miRNAs are listed in Table 1.

miRNAs differentially expressed between nonprogressing and progressing non–muscle-invasive tumors. To identify miRNAs for predicting subsequent disease progression to a muscle-invasive stage, we compared nonprogressing with progressing tumors and identified the most significantly regulated miRNAs using SAM (5% FDR as cutoff). Thirteen miRNAs were found to be significantly differentially expressed between the

groups (Fig. 1*B*; Table 2). Notably, the level of expression of miRNAs in progressing non–muscle-invasive samples resembled the level observed in the muscle-invasive tumors. Kaplan-Meier graphs of some of the most significantly regulated miRNAs (i.e., miR-129, miR-133b, miR-518c*, and miR-29c) are shown in Fig. 2. Optimal cutoff limits were determined for these miRNAs using receiver operating characteristic (ROC) curves (results not shown). Multivariate Cox regression analysis showed that all four miRNAs were significantly associated with disease progression [miR-133b: hazard ratio (HR), 3.5; $P = 0.002$; miR-518c*: HR, 3.2; $P = 0.003$; miR-129: HR, 3.0; $P < 0.02$; miR-29c: HR, 2.1; $P < 0.05$] when correcting for disease stage and grade. Combinations using miR-133b + miR-518c* and miR-133b + miR-129 showed an even better prediction of outcome (Fig. 2, *bottom row*). Multivariate Cox regression analysis of the combined miR-129 and miR-133b measure resulted in a HR of 9.2 ($P < 0.001$) when comparing the miR-129+/miR-133b+ group with the miR-129−/miR-133b− group. For the miR-129/miR-518c* combination, the multivariate Cox regression analysis showed a HR of 7.3 ($P < 0.001$).

To validate the robustness of miRNAs for outcome prediction, we performed leave-one-out cross-validation (LOOCV) using a maximum likelihood classifier approach as previously described (27). Optimal classification performance was achieved using six miRNAs in each cross-validation step. This gave a robust

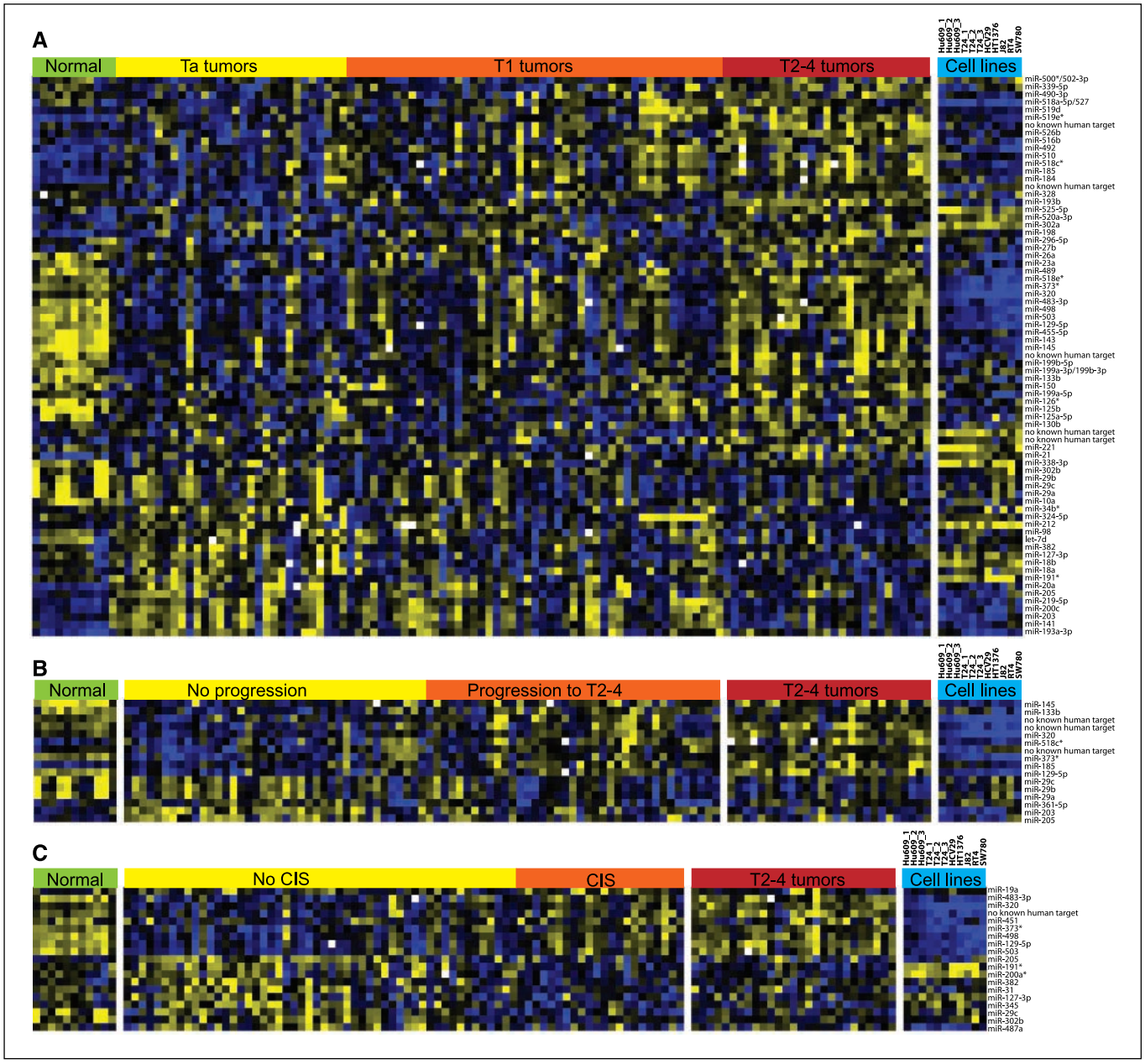

Figure 1. Expression patterns of miRNAs found to be significantly differentially expressed. *Yellow,* up-regulation of the miRNA; *blue,* down-regulation of the miRNA; *black,* median expression of the miRNA. All marker sets (*A–C*) were clustered hierarchically to align similar profiles. *A,* expression of the 73 miRNAs identified to show a significant difference between normal, Ta, T1, and T2-4 tumors. *B,* expression patterns of the 13 identified miRNAs significantly differentially expressed between nonprogressing and progressing tumors. *C,* expression patterns of the 18 identified miRNAs significantly differentially expressed between tumors with and without concomitant CIS.

separation of the classes with a sensitivity of 76% and a specificity of 75%. miR-133b, miR-29b, miR-29c, miR-361, miR-129, and miR-518c* were included in >90% of the cross-validation steps. Furthermore, as independent validation is crucial with multimarker studies, we divided the data into 100 independent training and validation sets (two thirds for training and one third for validation), identified optimal miRNAs for each training set, and used these for predicting outcome for each test set, respectively, as previously described (28). Using this approach, we obtained an average sensitivity of 63% and an average specificity of 66%, which is comparable with findings with mRNA transcripts (29). This approach identified the same set of miRNA as the LOOCV approach when selecting miRNAs used in >50% of the training sets. To validate the significance of the classifications, we generated random data and performed a similar selection and classification procedure. We found the classifications highly significant as none of the 100 random data sets generated an error rate that was below the average error rate for the real data set.

miRNAs differentially expressed between non–muscle-invasive tumors with and without concomitant CIS. Several patients included in this study were diagnosed with CIS in selected site biopsies at the present visit or at later cystoscopy examinations (for details, see Supplementary Table S3). We used SAM (5% FDR as cutoff) to identify miRNAs differentially expressed in tumors with or without CIS in selected site biopsies and identified 18 miRNAs with significant differential expression between the two groups of tumors (Fig. 1*C*; Table 2). As with the progression markers, the miRNA expression in non–muscle-invasive tumors with concomitant CIS resembles the expression observed for the muscle-invasive cases. Optimal cutoff limits for dichotomous analysis were determined for the most significant miRNAs using ROC curves (results not shown). Multivariate logistic regression analysis showed that the miRNA expressions were significantly associated with CIS status [miR-503: odds ratio (OR), 5.6; $P = 0.004$; miR-205: OR, 3.8; $P < 0.04$; miR-382: OR, 3.2; $P = 0.02$; miR-191: OR, 2.2; $P < 0.04$] when correcting for disease stage and grade. Again, comparing the miR-503+/miR-205+ group with the miR-503−/miR-205− group by multivariate logistic regression analysis gave an OR of 10.6 ($P = 0.006$) when adjusting for stage and grade. Other combinations gave similar high ORs (results not shown). The best classifier for CIS diagnosis was obtained using 44 miRNAs in LOOCV. This resulted in a sensitivity of 71% and a specificity of 72%. Unfortunately, the study did not include enough samples with concomitant CIS to perform an independent validation of the CIS-related miRNAs using the same approach as described above.

Real-time reverse transcription-PCR validation of miRNA expression. The microarray probes hybridize to both pri-, pre-, and mature forms of the miRNAs. Therefore, we investigated the relationship between expression of the mature form of nine miRNAs measured by real-time reverse transcription-PCR assays and the microarray data. The assays showed an average Pearson correlation to the microarray data of 0.8 (range, 0.6-0.9; Supplementary Fig. S2). This indicates that we mainly measure the mature miRNA in the clinical samples.

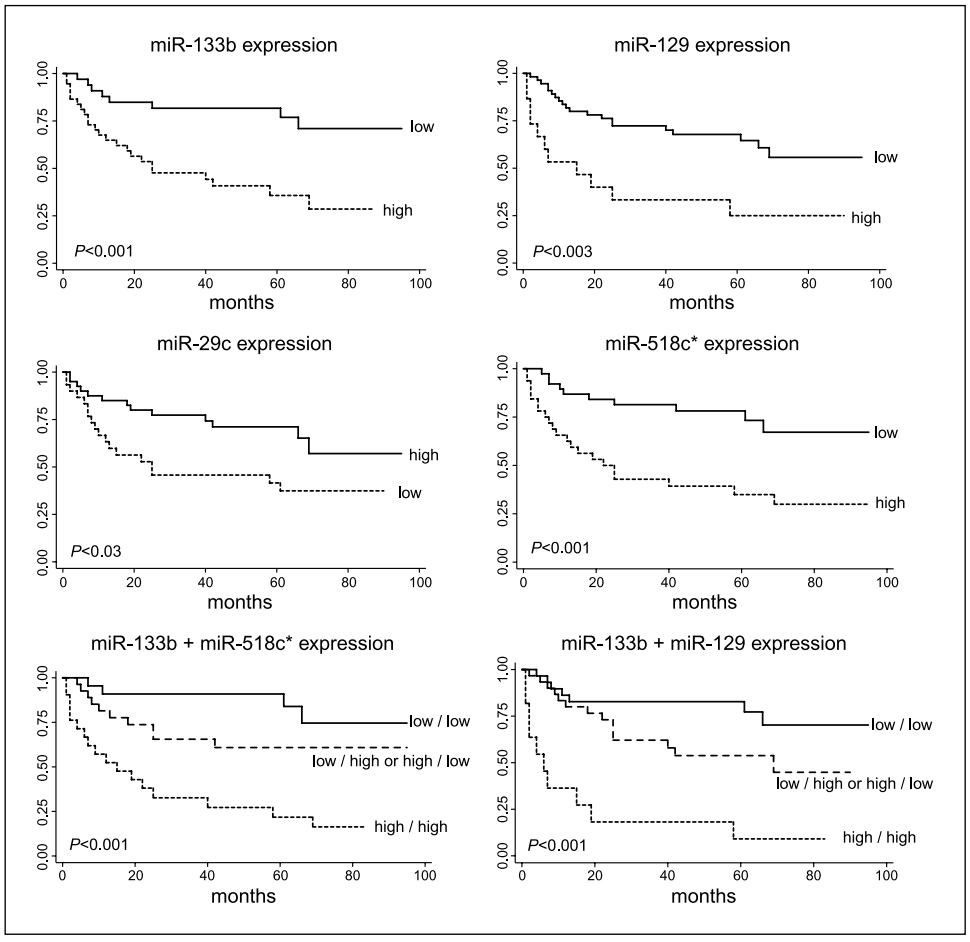

Figure 2. Kaplan-Meier plots of progression-free survival as a function of the expression of miR-133b, miR-129, miR-29c, miR-518c*, miR-133b + miR-518c*, and miR-133b + miR-129. Optimal cutoff points were determined for each miRNA using ROC curves to categorize the expressions into low and high groups. Log-rank test results are displayed for each Kaplan-Meier plot.

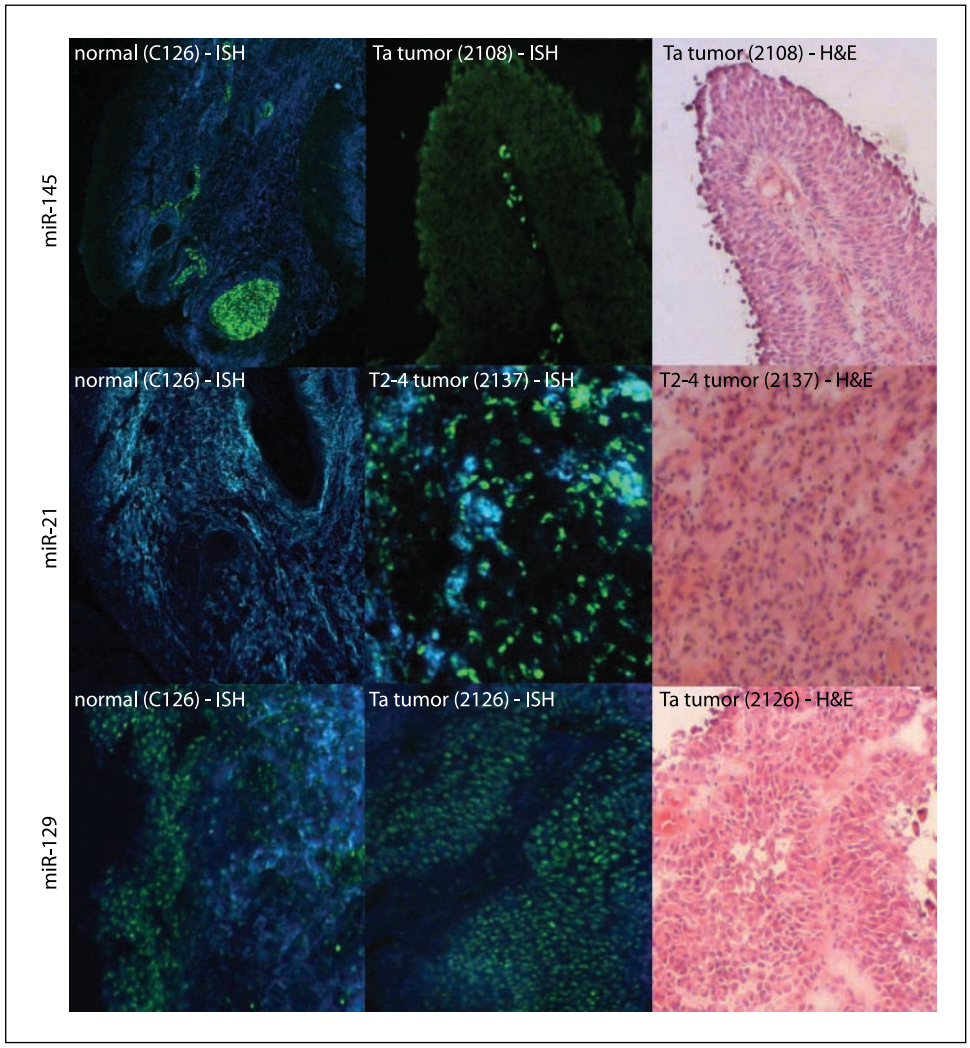

Figure 3. *In situ* hybridization for localization of miR-145, miR-21, and miR-129 expression in normal urothelium and in tumor tissue. *Right,* H&E-stained overview sections of tumor tissues. Images are overlay images with blue color representing DAPI staining and green color representing miRNA expression (except for miR-145 tumor image that only includes the miRNA expression). The sections for *in situ* hybridization and for H&E staining are consecutive sections, not identical sections.

Localization of miRNA expression by *in situ* hybridization. We used FITC-labeled LNA oligonucleotide probes for detection of miR-145, miR-21, and miR-129 expression (Fig. 3). Expression of miR-145 was identified in connective tissue, endothelial cells, and infiltrating lymphocytes; varying expression, lowest in cancer, was detected in normal urothelium or in urothelial carcinoma cells. Expression of miR-21 was not detected in normal tissue biopsies. In tumor tissue, we identified the expression of miR-21 to be located in the carcinoma cells. miR-129 expression was detected both in the normal urothelial cells and in the carcinoma cells in tumor tissue.

Functional characterization of miR-129 and miR-21. miR-129 and miR-21 were selected for functional characterization as they showed prognostic and diagnostic potential, respectively. We evaluated the function of miR-129 by transfecting T24 and SW780 cells with a synthetic miR-129 precursor (pre-miR-129). The miRNA precursor molecules are processed by the cellular miRNA machinery into mature miRNAs. Pre-miR-129 transfection resulted in a profound antiproliferative effect as determined by a MTT assay. Furthermore, pre-miR-129 transfection was accompanied by induction of cell death as determined by phase-contrast microscopy and LDH release assay (Fig. 4; data not shown). We investigated this further by profiling gene expression and miRNA expression at 24- and 48-hour time points following transfection of T24 cells with 10 nmol/L pre-miR-129 or scrambled sequence. miRNA profiling verified the transfection efficacy by showing a 1.5-fold miR-129 up-regulation after 24 hours and a 2-fold up-regulation after 48 hours. No other miRNAs were significantly differentially expressed (>2-fold) following pre-miR-129 transfection. Gene expression microarray data were analyzed using IPA software and gene networks were generated from gene expression changes at 24- and 48-hour time points following transfection. The results obtained from IPA identify cellular networks of identified molecules and not molecular pathways. However, the top gene networks were associated with the functional categories: cell death, cancer, and cellular growth and proliferation (24-hour time point) and cell death, inflammatory disease, and cancer (48-hour time point). Knockdown of endogenous miR-129 by LNA knockdown probes did not affect cell viability probably due to the low endogenous level of miR-129 in the cell lines (data not shown).

Transfection of T24 cells with a synthetic miR-21 precursor (pre-miR-21) and knockdown of endogenous miR-21 by LNA knockdown probes did not lead to a phenotype change (results not shown). Transfection efficacy was successfully verified by quantitative PCR and the functionality of the transfection was

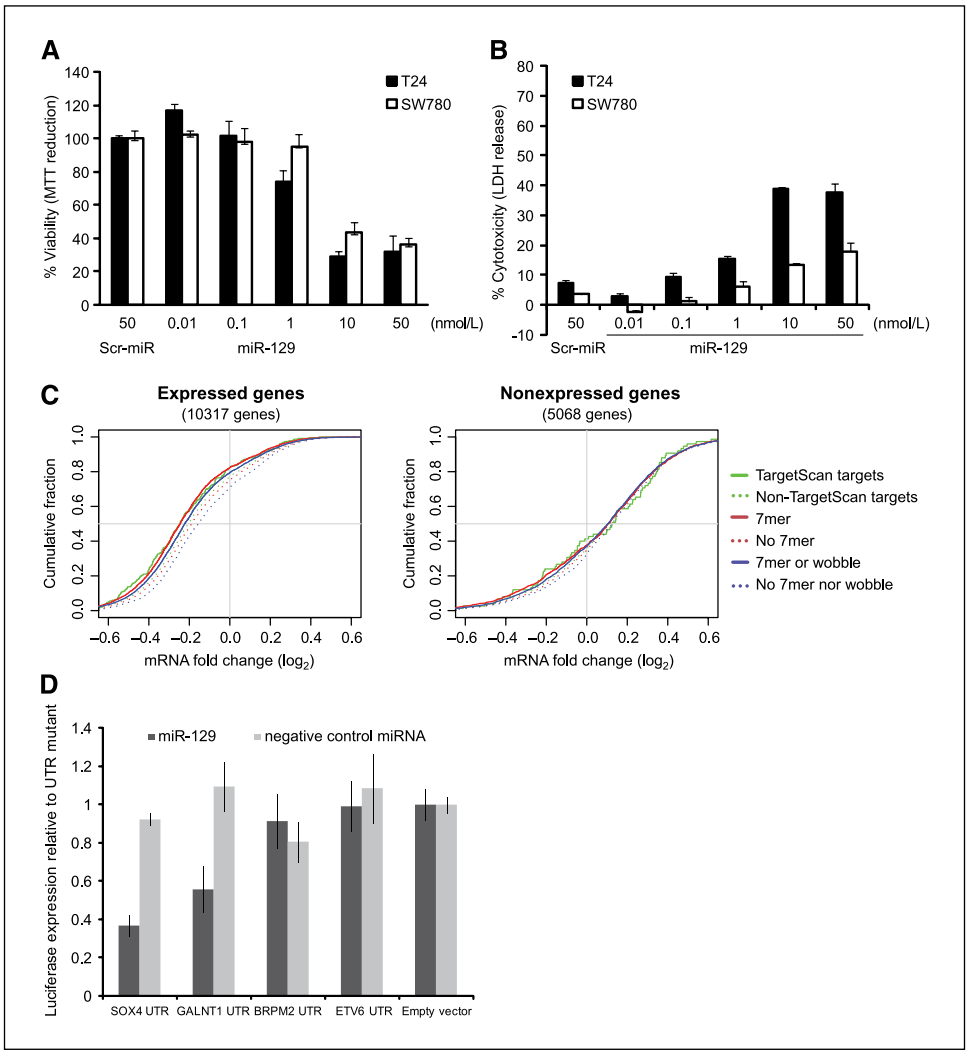

Figure 4. Transfection of miR-129 in T24 and SW780 cells. Cells were transfected with 50 nmol/L scrambled (*Scr*) miRNA or the indicated concentrations of miR-129 precursor. *A,* the viability of the cells was determined 96 h after transfection by the MTT reduction assay and expressed as the viability compared with the scr-transfected control. *B,* the dose-dependent cell death was determined 96 h after transfection by the LDH release assay and expressed as the percentage of the released LDH of the total cellular LDH. *Columns,* averages of triplicate experiments; *bars,* SD. Data are representative of a minimum of three triplicate experiments. *C,* distribution of transcript regulations according to the presence of miR-129 target sites. *Left,* transcripts expressed above the background level determined from the expression in nontransfected T24 cells (>8; $\log_2$ scale); *right,* transcripts not expressed above the background level. Note that expressed genes with complementary miR-129 seed or target sequences are more down-regulated than genes without a complementary seed or target sequence. This effect is not observed for nonexpressed genes. *D,* validation of functional miR-129 target sites using partial UTR sequences from *SOX4, GALNT1, BRPM2*, and *ETV6* using luciferase reporter assays. Luciferase expression for each target gene is shown relative to the luciferase expression from reporters with mutated target sites.

successfully verified by evaluating changes of the miR-21 targets PDCD4 and SERPINB5 (Supplementary Fig. S3).

miRNA target expression and validation. We investigated the regulation of miR-129 targets in the microarray gene expression data generated and found a significant (P = 0.0002, χ^2 test) enrichment of miR-129 target genes among genes down-regulated 24 hours after pre-miR-129 transfection (Supplementary Table S4; Fig. 4*C*). This target effect was not significant 48 hours after transfection. However, at both time points, we observed a highly significant increase in the average number of complementary miR-129 seeds in the down-regulated transcripts compared with up-regulated and nonregulated transcripts (P < 0.00001, permutation analysis). Down-regulated targets are listed in Supplementary Table S5.

We used previously published human bladder cancer gene expression data sets to analyze changes in expression of mRNA target molecules of the identified miRNAs listed in Tables 1 and 2. We identified significantly regulated transcripts between the relevant groups (see Materials and Methods). By comparing the number of up-regulations/down-regulations of targets with non-targets, we found that for several of the miRNAs investigated there was a statistically significant higher number of differentially expressed miRNA targets compared with nontargets. For example, for miR-510 that was up-regulated in bladder cancer, a significantly higher proportion of the predicted miR-510 targets were down-regulated compared with nontargets. Thus, in the normal versus cancer comparison, the following miRNAs showed significant differences in regulation of targets versus nontargets: miR-510 (P = 0.004), miR-455-5p (P = 0.04), miR-143 (P = 0.01), miR-145 (P = 7.5E10−5), miR-126* (P = 0.005), and miR-26a (P = 0.003). We observed no significant overrepresentation of regulated targets for miRNAs differentially expressed between tumors with and without surrounding CIS and between Ta and T2-4 tumors. Interestingly, miR-129 targets were significantly overrepresented in the comparison between nonprogression and progression groups (P = 0.001). See Supplementary Table S6 for details. miR-129 targets FNDC3b, TP53INP1, ETV6, GALNT1, TNPO1, ZFP91, SCC-112, and BMPR2 were significantly down-regulated in non–muscle-invasive tumors with later progression. Next, we analyzed miR-129, target interactions for ETV6, GALNT1, BRPM2, and SOX4, using luciferase assays (Fig. 4*D*). GALNT1 was down-regulated at both time points in the *in vitro* pre-miR-129 transfection assay and SOX4 was down-regulated at the 48-hour time point only. We included SOX4, although it was not differentially expressed in the clinical samples analyzed. However, it has previously been associated with disease progression (30).

GALNT1 and SOX4 both showed significant reduction in luciferase activity on transfection with pre-miR-129 compared with GALNT1 and SOX4 3′-UTRs with mutated miR-129 target sites.

Discussion

Previously, no reports have described miRNA expression associated with clinical parameters and outcome in bladder cancer. One study has reported miRNAs differentially expressed between normal bladder mucosa and bladder tumors (9). However, a limited number of reference samples were analyzed (two samples of normal bladder mucosa), and this may explain the lack of overlap between the results presented here and the previously reported results.

Here, we profiled the expression of 290 miRNAs in bladder tumors, normal tissue, and various immortalized and cancerous bladder cell lines. We identified several miRNAs differentially expressed between normal and cancer and between the different stages of cancer. Furthermore, we identified miRNAs with potential prognostic potential for predicting disease progression, as they performed well in independent training and validation sets.

For prediction of progression, we built a molecular classifier and randomly divided our samples into 100 training and validation sets. This approach is advocated over the use of a single training and validation set as bias associated with selecting the samples only once is minimized. It has been shown that previous multimarker studies may have reported overoptimistic results because of the lack of using the multiple random validation strategy as used here (31).

Knowledge about the functional roles of specific miRNAs is steadily increasing; however, knowledge is still missing for a large part of the identified miRNAs in this work. Nevertheless, functional roles have been described for some of the most significant differentially expressed miRNAs in our study. We identified miR-21 to be significantly up-regulated 3.7-fold in bladder cancer, and we located the expression to the carcinoma cells, with no detection of miR-21 in normal urothelium. Up-regulation of miR-21 has been described in several other solid cancers as well (32). Interestingly, miR-21 has been reported to promote cell transformation in breast cancer cells (33), and it is involved in invasion in colorectal cancer cells (34). Depletion of miR-21 in breast cancer cell lines, furthermore, was shown to suppress cell growth and promote apoptosis (35). In addition, miR-21 targets the tumor suppressor genes TPM1 (36) and PTEN (37). Notably, here, we performed miR-21 overexpression and depletion in bladder cancer T24 cells and did not observe a change in cell growth or apoptosis in this cell line. However, this lack of phenotypic change may be cell type specific, especially when considering the phenotype changes observed for other cell lines. Among the most significantly down-regulated miRNAs, we found miR-143 (2.6-fold) and miR-145 (7.0-fold). However, miR-145 expression was predominantly associated with connective tissue and lymphocytes. Minimal expression was detected in carcinoma cells and normal urothelial cells. miR-145 and miR-143 have also been reported to be down-regulated in other cancers (32, 38), and miR-145 has been reported to suppress cell growth in cervical and colorectal cancer cell lines (19, 39). Other interesting down-regulated miRNAs are miR-455-5p located at chromosome 9q32 and miR-126* located at chromosome 9q34, a region commonly lost in early stages of bladder cancer (40). However, at present, little is known about these two miRNAs. In muscle-invasive tumors, progressing non–muscle-invasive tumors, and tumors with concomitant CIS, we identified miR-129 to be significantly up-regulated. Using *in situ* hybridization, we localized the miR-129 expression to the carcinoma cells and to the normal urothelial cells. In one report, it is described that miR-129 targets TAMTA1 and EIF2CA, genes related to miRNA processing or transcription regulation (41). Here, we showed that transfection of T24 and SW780 cells with miR-129 precursor resulted in decreased cell viability and induction of cell death. Obviously, the cells are not dying in progressing and muscle-invasive tumors, indicating that defects in the downstream death effector pathways of miR-129 expression must arise in progressing tumors, similar to previous findings with SOX4 (30). Among the miRNAs down-regulated in invasive tumors compared with non–muscle-invasive tumors, we identified miR-200c and miR-141 from the miR-200 family. It has been shown that miR-200c and miR-141 are down-regulated in cells that have undergone epithelial to mesenchymal transition (EMT). The miRNAs regulate ZEB1 and SIP1, which are proteins directly involved in EMT and tumor metastases (42). miR-320a was identified to be significantly differentially expressed in progressing tumors and in tumors with surrounding CIS. In the tumors with surrounding CIS, we also identified miR-498 to be significantly differentially expressed. Interestingly, these two miRNAs have been reported recently to be associated with tumor relapse in colorectal cancer (19). We found the miR-29 family to be significantly down-regulated in progressing tumors. The miR-29 family has been reported to regulate the apoptotic protein MCL1 and thereby regulating apoptosis (43) as well as DNA *de novo* methyltransferases DNMT3A and DNMT3B, key enzymes that are frequently up-regulated in cancer (44).

Because miRNAs exert their function through both translational repression and degradation of mRNA targets, we did not expect a high degree of correlation between miRNA expression and target expression. However, we analyzed target regulation in previously generated gene expression data from bladder tumors. For some of the identified miRNAs, we found a significant overrepresentation of differentially expressed target transcripts compared with nontarget transcripts. The effect was most pronounced for the miRNAs differentially expressed between normal and cancer probably because the differences were most significant in this comparison. Interestingly, we observed that transcripts down-regulated in progressing samples in concert with the up-regulation of miR-129 were significantly enriched for miR-129 target sites. We also observed enrichment for miR-129 target sites in down-regulated transcripts *in vitro* following T24 cell transfection with miR-129 precursor. Among the down-regulated miR-129 targets, we found TP53INP1, which has been shown to have a tumor suppressor function in melanoma (45), and BMPR2, which has been reported to be associated with development of colorectal cancer (46). We showed that the down-regulated targets SOX4 and GALNT1 were direct targets for miR-129 in luciferase assays. A high level of SOX4 has previously been described to be associated with increased survival for bladder cancer patients (30). This correlates well with our finding that high levels of miR-129 (and corresponding low SOX4 levels) are correlated to progression and thus most probably a poor outcome. Furthermore, GALNT1 has been shown to have an important role in transforming growth factor-β signaling (47).

In conclusion, we showed that in bladder cancer, several miRNAs are significantly differentially expressed according to histopathologic and clinical parameters. The miRNAs identified in this study may serve as candidate biomarkers for diagnostic and prognostic purposes with respect to treatment stratification in the future.

Disclosure of Potential Conflicts of Interest

No potential conflicts of interest were disclosed.

Acknowledgments

Received 10/21/08; revised 3/10/09; accepted 3/28/09.

Grant support: The John and Birthe Meyer Foundation, The Danish Cancer Society, the Ministry of Technology and Science, the Lundbeck Foundation, and the EU FP7 framework. Wilhelm Johannsen Centre for Functional Genome Research is established by the Danish National Research Foundation.

The costs of publication of this article were defrayed in part by the payment of page charges. This article must therefore be hereby marked *advertisement* in accordance with 18 U.S.C. Section 1734 solely to indicate this fact.

We thank Gitte Høj, Pamela Celis, Hanne Steen, Inge Lis Thorsen, Gitte Stougård, and Conni Sørensen for technical assistance and the staff at the Departments of Urology, Clinical Biochemistry, and Pathology at Aarhus University Hospital.

References

1. Cookson MS, Herr HW, Zhang ZF, Soloway S, Sogani PC, Fair WR. The treated natural history of high risk superficial bladder cancer: 15-year outcome. J Urol 1997;158:62–7.
2. Dyrskjot L, Zieger K, Orntoft TF. Recent advances in high-throughput molecular marker identification for superficial and invasive bladder cancers. Front Biosci 2007;12:2063–73.
3. Iorio MV, Ferracin M, Liu CG, et al. MicroRNA gene expression deregulation in human breast cancer. Cancer Res 2005;65:7065–70.
4. Lee EJ, Gusev Y, Jiang J, et al. Expression profiling identifies microRNA signature in pancreatic cancer. Int J Cancer 2007;120:1046–54.
5. Michael MZ, O' Connor SM, van Holst Pellekaan NG, Young GP, James RJ. Reduced accumulation of specific microRNAs in colorectal neoplasia. Mol Cancer Res 2003;1:882–91.
6. Yanaihara N, Caplen N, Bowman E, et al. Unique microRNA molecular profiles in lung cancer diagnosis and prognosis. Cancer Cell 2006;9:189–98.
7. Ciafre SA, Galardi S, Mangiola A, et al. Extensive modulation of a set of microRNAs in primary glioblastoma. Biochem Biophys Res Commun 2005;334:1351–8.
8. Murakami Y, Yasuda T, Saigo K, et al. Comprehensive analysis of microRNA expression patterns in hepatocellular carcinoma and non-tumorous tissues. Oncogene 2006;25:2537–45.
9. Gottardo F, Liu CG, Ferracin M, et al. Micro-RNA profiling in kidney and bladder cancers. Urol Oncol 2007;25:387–92.
10. Neely LA, Rieger-Christ KM, Neto BS, et al. A microRNA expression ratio defining the invasive phenotype in bladder tumors. Urol Oncol. In press 2009.
11. Calin GA, Croce CM. MicroRNA signatures in human cancers. Nat Rev Cancer 2006;6:857–66.
12. Calin GA, Dumitru CD, Shimizu M, et al. Frequent deletions and down-regulation of micro-RNA genes miR15 and miR16 at 13q14 in chronic lymphocytic leukemia. Proc Natl Acad Sci U S A 2002;99:15524–9.
13. Cimmino A, Calin GA, Fabbri M, et al. miR-15 and miR-16 induce apoptosis by targeting BCL2. Proc Natl Acad Sci U S A 2005;102:13944–9.
14. Tavazoie SF, Alarcon C, Oskarsson T, et al. Endogenous human microRNAs that suppress breast cancer metastasis. Nature 2008;451:147–52.
15. Calin GA, Ferracin M, Cimmino A, et al. A microRNA signature associated with prognosis and progression in chronic lymphocytic leukemia. N Engl J Med 2005;353:1793–801.
16. Rosenfeld N, Aharonov R, Meiri E, et al. MicroRNAs accurately identify cancer tissue origin. Nat Biotechnol 2008;26:462–9.
17. Bergkvist A, Ljungqvist A, Moberger G. Classification of bladder tumours based on the cellular pattern. Preliminary report of a clinical-pathological study of 300 cases with a minimum follow-up of eight years. Acta Chir Scand 1965;130:371–8.
18. Foghsgaard L, Wissing D, Mauch D, et al. Cathepsin B acts as a dominant execution protease in tumor cell apoptosis induced by tumor necrosis factor. J Cell Biol 2001;153:999–1010.
19. Schepeler T, Reinert JT, Ostenfeld MS, et al. Diagnostic and prognostic microRNAs in stage II colon cancer. Cancer Res 2008;68:6416–24.
20. Saeed AI, Sharov V, White J, et al. TM4: a free, open-source system for microarray data management and analysis. Biotechniques 2003;34:374–8.
21. Thorsen K, Sorensen KD, Brems-Eskildsen AS, et al. Alternative splicing in colon, bladder, and prostate cancer identified by exon-array analysis. Mol Cell Proteomics 2008;7:1214–24.
22. Aaboe M, Marcussen N, Jensen KM, Thykjaer T, Dyrskjot L, Orntoft TF. Gene expression profiling of noninvasive primary urothelial tumours using microarrays. Br J Cancer 2005;93:1182–90.
23. Dyrskjot L, Kruhoffer M, Thykjaer T, et al. Gene expression in the urinary bladder: a common carcinoma *in situ* gene expression signature exists disregarding histopathological classification. Cancer Res 2004;64:4040–8.
24. Dyrskjot L, Zieger K, Kruhoffer M, et al. A molecular signature in superficial bladder carcinoma predicts clinical outcome. Clin Cancer Res 2005;11:4029–36.
25. Lewis BP, Shih IH, Jones-Rhoades MW, Bartel DP, Burge CB. Prediction of mammalian microRNA targets. Cell 2003;115:787–98.
26. Krek A, Grun D, Poy MN, et al. Combinatorial microRNA target predictions. Nat Genet 2005;37:495–500.
27. Dyrskjot L, Thykjaer T, Kruhoffer M, et al. Identifying distinct classes of bladder carcinoma using microarrays. Nat Genet 2003;33:90–6.
28. Kruhoffer M, Jensen JL, Laiho P, et al. Gene expression signatures for colorectal cancer microsatellite status and HNPCC. Br J Cancer 2005;92:2240–8.
29. Dyrskjot L, Zieger K, Real FX, et al. Gene expression signatures predict outcome in non-muscle-invasive bladder carcinoma: a multicenter validation study. Clin Cancer Res 2007;13:3545–51.
30. Aaboe M, Birkenkamp-Demtroder K, Wiuf C, et al. SOX4 expression in bladder carcinoma: clinical aspects and *in vitro* functional characterization. Cancer Res 2006;66:3434–42.
31. Michiels S, Koscielny S, Hill C. Prediction of cancer outcome with microarrays: a multiple random validation strategy. Lancet 2005;365:488–92.
32. Volinia S, Calin GA, Liu CG, et al. A microRNA expression signature of human solid tumors defines cancer gene targets. Proc Natl Acad Sci U S A 2006;103:2257–61.
33. Lu Z, Liu M, Stribinskis V, et al. MicroRNA-21 promotes cell transformation by targeting the programmed cell death 4 gene. Oncogene 2008;27:4373–9.
34. Asangani IA, Rasheed SA, Nikolova DA, et al. MicroRNA-21 (miR-21) post-transcriptionally downregulates tumor suppressor Pdcd4 and stimulates invasion, intravasation and metastasis in colorectal cancer. Oncogene 2008;27:2128–36.
35. Si ML, Zhu S, Wu H, Lu Z, Wu F, Mo YY. miR-21-mediated tumor growth. Oncogene 2007;26:2799–803.
36. Zhu S, Si ML, Wu H, Mo YY. MicroRNA-21 targets the tumor suppressor gene tropomyosin 1 (TPM1). J Biol Chem 2007;282:14328–36.
37. Meng F, Henson R, Wehbe-Janek H, Ghoshal K, Jacob ST, Patel T. MicroRNA-21 regulates expression of the PTEN tumor suppressor gene in human hepatocellular cancer. Gastroenterology 2007;133:647–58.
38. Slaby O, Svoboda M, Fabian P, et al. Altered expression of miR-21, miR-31, miR-143 and miR-145 is related to clinicopathologic features of colorectal cancer. Oncology 2007;72:397–402.
39. Wang X, Tang S, Le SY, et al. Aberrant expression of oncogenic and tumor-suppressive microRNAs in cervical cancer is required for cancer cell growth. PLoS ONE 2008;3:e2557.
40. Knowles MA. Molecular pathogenesis of bladder cancer. Int J Clin Oncol 2008;13:287–97.
41. Liao R, Sun J, Zhang L, et al. MicroRNAs play a role in the development of human hematopoietic stem cells. J Cell Biochem 2008;104:805–17.
42. Gregory PA, Bert AG, Paterson EL, et al. The miR-200 family and miR-205 regulate epithelial to mesenchymal transition by targeting ZEB1 and SIP1. Nat Cell Biol 2008;10:593–601.
43. Mott JL, Kobayashi S, Bronk SF, Gores GJ. mir-29 regulates Mcl-1 protein expression and apoptosis. Oncogene 2007;26:6133–40.
44. Fabbri M, Garzon R, Cimmino A, et al. MicroRNA-29 family reverts aberrant methylation in lung cancer by targeting DNA methyltransferases 3A and 3B. Proc Natl Acad Sci U S A 2007;104:15805–10.
45. Bonazzi VF, Irwin D, Hayward NK. Identification of candidate tumor suppressor genes inactivated by promoter methylation in melanoma. Genes Chromosomes Cancer 2009;48:10–21.
46. Beppu H, Mwizerwa ON, Beppu Y, et al. Stromal inactivation of BMPRII leads to colorectal epithelial overgrowth and polyp formation. Oncogene 2008;27:1063–70.
47. Herr P, Korniychuk G, Yamamoto Y, Grubisic K, Oelgeschlager M. Regulation of TGF-β signalling by N-acetylgalactosaminyltransferase-like 1. Development 2008;135:1813–22.